

A Novel Nanocomposite With Photo-Polymerization for Wafer Level Application

Yangyang Sun, *Student Member, IEEE*, Hongjin Jiang, Lingbo Zhu, and C. P. Wong, *Fellow, IEEE*

Abstract—A novel nanocomposite photo-curable material which can act both as a photoresist and a stress redistribution layer applied on the wafer level was synthesized and studied. In the experiments, 20-nm silica fillers were modified by a silane coupling agent through a hydrolysis and condensation reaction and then incorporated into the epoxy matrix. A photo-sensitive initiator was added into the formulation which can release cations after ultraviolet exposure and initiate the epoxy crosslinking reaction. The photo-crosslinking reaction of the epoxy made it a negative tone photoresist. The curing reaction of the nanocomposites was monitored by a differential scanning calorimeter with the photo-calorimetric accessory. The thermal mechanical properties of photo-cured nanocomposites thin film were also measured. It was found that the moduli change of the nanocomposites as the filler loading increasing did not follow the Mori-Tanaka model, which indicated that the nanocomposite was not a simple two-phase structure as the composite with micron size filler. The addition of nano-sized silica fillers reduced the thermal expansion and improved the stiffness of the epoxy, with only a minimal effect on the optical transparency of the epoxy, which facilitated the complete photo reaction in the epoxy.

Index Terms—Nanocomposite, photo polymerization, thermal expansion, wafer level packaging.

I. INTRODUCTION

WITH the fast development of electronics industry, electronics products are becoming smaller, faster with more functionality, higher performance, and lower cost. The technical advances have entered into the nano-scale threshold with the decreasing of feature size and increasing input/output (I/O) number in the integrated circuit (IC) chip. New interconnection technology such as wafer level packaging has been invented to meet these trends [1]. Here, we report on the development of a novel photo-definable material which can act both as a photoresist and as a stress redistribution layer applied on the wafer level. In the proposed process, this material is applied on the un-bumped wafer, and then is exposed to ultraviolet (UV) light through a mask for crosslinking. After development, the un-exposed material is removed and the bump pads on the wafer are

Manuscript received October 5, 2005; revised November 4, 2006. This work was supported by the Packaging Research Center, Georgia Institute of Technology. This work was recommended for publication by Associate Editor J. Morris upon evaluation of the reviewers comments.

Y. Sun, H. Jiang, and C. P. Wong are with the School of Materials Science and Engineering, Packaging Research Center, Georgia Institute of Technology, Atlanta GA 30332 USA (e-mail: cp.wong@mse.gatech.edu).

L. Zhu is with the School of Chemical and Biomolecular Engineering, Packaging Research Center, Georgia Institute of Technology, Atlanta GA 30332 USA.

Color versions of one or more of the figures in this paper are available online at <http://ieeexplore.ieee.org>.

Digital Object Identifier 10.1109/TCAPT.2008.916809

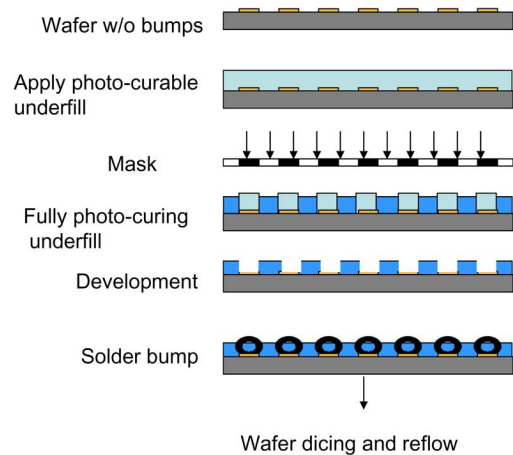


Fig. 1. Proposed wafer process with novel photo-definable nanocomposite.

exposed for solder bumping. The fully cured material film is left on the wafer for protection of the bumps. Fig. 1 shows the proposed process.

The proposed wafer-level underfill application requires an underfill material with high photo-reactivity, low CTE, good chemical resistance and good mechanical properties. Epoxy resins have been extensively used in electronic packaging industry due to their extreme versatility in chemical structures, less curing shrinkage, excellent adhesion and chemical resistance. However, the coefficient of thermal expansion (CTE) mismatch between the neat epoxy resin (50–80 ppm/K) and the silicon (2.8 ppm/K) causes a large amount of stress at the interface. This stress effect is pronounced in the large area application on the whole wafer [2]. The introduction of well-dispersed inorganic particles into a polymer matrix has been demonstrated to be extremely effective in improving the performance of the polymer composites [3]. Because of the exceptionally low CTE of fused SiO₂ (silica) due to the high Si–O bond energy, silica filled composite materials have been widely used to improve the mechanical properties [4], [5] and reduce the CTE of epoxy [6].

In the recent years, a number of investigations have demonstrated the feasibility of photo-polymerization for polymers and their composites. These polymers can be classified into two categories, depending on whether the polymerization proceeds by a free radical-type or cationic-type reaction center. The first case is based on the vinyl compounds [7] or acrylate compounds [8] initiated by free radical reaction. Free radical-type systems are by far the most widely used and studied in today's photo curing application due to their high reactivity. The second case is based on photoinitiated cationic polymerization. A proton

acid is produced by photolysis of triarylsulfonium (TAS) or diaryliodonium salt to initiate the polymerization of the epoxide ring. Utilizing this reaction technique, the Bisphenol-A novolac epoxy resin (EPON SU-8) has been used as a negative near-UV photoresist in a microelectromechanical systems (MEMS) fabrication process [9], as well as polymer optical waveguide materials [10]. Previous research about the conductive adhesive had demonstrated the application of the dual initiators including both the photo initiator and the thermal initiator for the cycloaliphatic epoxy based conductive adhesives [11]. The adhesive can be cured quickly at ambient temperature by the cationic polymerization after UV exposure, then the thermal initiator can fully cure the adhesive at elevated temperature and eliminate the disadvantage of the inherent lack of transparency caused by the metal particles in the adhesives. Nevertheless, there are few reports of the photo-polymerization of silica/epoxy composites via the cationic crosslinking reaction because micron size silica fillers can scatter UV light and hinder photo-polymerization process. Nanosilica composites, on the other hand, have displayed desirable optical properties [12], [13] and have become the best solution for photo-definable applications.

In this paper, photo-definable materials based on nanosilica and epoxy were synthesized. A photo-sensitive initiator was added into the formulation which can release cations after UV exposure and initiate the epoxy crosslinking reaction. The photo-crosslink reaction of the epoxy makes it a negative tone photoresist. A comprehensive study of the photo-curing behaviors of these materials was conducted to elucidate the photo-polymerization mechanism in the composites and achieve an in-depth understanding of the effect of nanosilica on the photo-reaction of epoxy. Thermal and mechanical properties were also determined and the data used to optimize the formulation of a photo-definable nanocomposite for wafer level applications.

II. EXPERIMENTAL

1) *Materials*: Colloidal nanosilica with average size of 20 nm was synthesized by the sol-gel method. The size was characterized by the transmission electron microscopy (TEM). EPON 862, a Bisphenol F epoxy, was obtained from Shell Chemicals. The photoinitiator, KI85, was obtained from Sartomer.

2) *Preparation of Nanocomposites*: The nanosilica was modified by the proper silane coupling agent following the method described before [14] and then incorporated into the epoxy matrix. After surface modification, nanosilica interacted with the polymer matrix and can achieve a high filler loading level. The nanosilica filler loadings in the epoxy matrix were 10 wt%, 20 wt%, 30 wt%, and 40 wt%. The photoinitiator KI85 (2mol%) was added into the formulations and the mixtures were stirred one hour.

3) *Characterization*: The photo absorption properties of the samples were measured with a UV-Visible spectrophotometer (Beckman Du520). The absorption of the photoinitiator and the colloidal silica was characterized in an ethanol solution. To measure the absorption of photo-definable nanocomposites, liquid composites were spin-coated on a quartz glass slide. Then the

specimen was put into the chamber of the UV-Vis spectrophotometer and scanned.

The curing process of the photo-definable nanocomposite materials was characterized by a photo differential scanning calorimeter (DSC). The photo-DSC was performed using a Q1000 DSC (TA Instruments) equipped with the photo calorimeter accessory (PCA). The wavelength of the UV light was 320–500 nm and its intensity was approximately 20 mW/cm². Reactions were performed at room temperature in a nitrogen atmosphere. Sample sizes were around 10 mg. The residual reaction heat and glass transition temperature of the photo-definable nanocomposites after UV exposure were characterized by the DSC. A dynamic scanning experiment was conducted with a ramp rate of 5 °C/min, from ambient temperature to 300 °C. The cured sample was left in the DSC cell and cooled to room temperature. Then the sample was reheated to 200 °C at 5 °C/min to obtain another heat flow diagram in the modulated mode. The initial temperature of the heat flow step of the second diagram is defined as the glass transition temperature (DSC Tg).

In order to evaluate material properties of the nanocomposite samples after UV curing, the liquid nanocomposites were cast onto an aluminum substrate with a thickness around 50 μm. UV curing of samples was performed using a UV lamp (CLE-4001, with a long-wave UVA portion of the spectrum) for 20 min. The intensity was ~ 50 mW/cm² measured by a traceable radiometer. Curing of samples were performed in the air. Then the sample was thermally cured at 95 °C for 30 minutes to complete the crosslinking reaction. Samples were peeled off from the aluminum substrate yielding free-standing nanocomposite films for further characterization.

A Dynamic Mechanical Analyzer (DMA, TA Instruments, Model 2980) was used to measure the dynamic moduli and glass transition temperature of the nanocomposites. The cured film was cut into a strip of dimensions about 18 × 6 mm. The accurate thickness of the film was measured by a laser profilometer. The test was performed in the film mode. The temperature was increased from room temperature to 250 °C at a heating rate of 3 °C/min, while the storage modulus (E'), loss modulus (E'') and tan δ were calculated by the pre-installed software. In order to obtain complementary measurements to the DSC, the DMA Tg was determined by the peak temperature of the tan delta (tan δ) curve.

The coefficient of thermal expansion (CTE) of the cured film was measured on a Thermo-Mechanical Analyzer (TMA, TA Instruments, Model 2940). The dimensions of the sample were about 10 × 5 mm. The samples were heated in the TMA furnace at 5 °C/min from room temperature to 200 °C. The CTE before the Tg is defined as α₁ and after the Tg as α₂.

The thermal stability of the sample was characterized by a Thermogravimetric Analyzer (TGA, TA Instruments, Model 2050). The cured samples were put into a TGA pan. The experiment was conducted with a ramp rate of 20 °C/min from ambient temperature to 800 °C in air.

The dispersion and morphology of the nanocomposite after photo curing were characterized by transmission electron microscopy (TEM). The cross sections of the nanocomposite were prepared using a Leica Microtome Nova. The samples were first

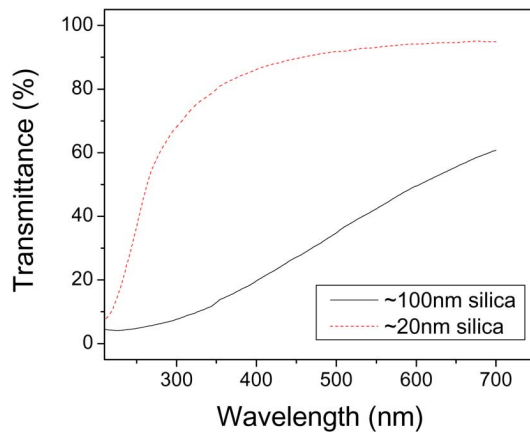


Fig. 2. Light transmittance of two kinds of nanosize silica in ethanol solution.

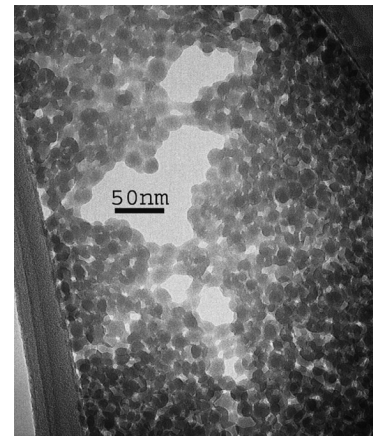


Fig. 3. TEM picture of the 20 nm colloidal silica.

trimmed manually using a razor blade to produce a trapezoidal cross section with an area that was approximately 0.5mm by 0.5mm. The samples were then mounted on the microtome and aligned with a glass knife, which was used to trim the sample further. Each sample was trimmed until its surface was parallel to the glass. The glass knife was then replaced with a diamond knife, which was used to make the final sections. The final thickness of the sections was between 30–60 nm and they were mounted on a copper TEM grid. The TEM investigations were performed on a JEOL 100CX TEM operating at an acceleration voltage of 100 KV.

III. RESULTS AND DISCUSSIONS

A. Preparation of Photo-Curable Nanocomposites

Previous research on silica/epoxy nanocomposites has shown that the addition of nanosilica was small enough to not disturb the optical transparency of the composite materials in the visible light range [13], [15]. Nevertheless, the 100 nm silica significantly scatters the UV light at the wavelength region which excites the cationic initiators for the photo-polymerization of epoxy. Therefore, even smaller size silica is needed for photo curing applications. 20 nm silica can be synthesized in the colloidal form by the sol-gel method. The transmittance of these two types of nanosilica filler in the ethanol solution is measured by UV-Visible spectroscopy as shown in Fig. 2. It can be seen that the 20 nm silica has > 95% transmittance in the UV to visible light region, which is much better than the 100 nm silica. Therefore, the 20 nm silica was chosen as the filler in the composite due to its good transparency to UV light. (Hereafter, the term nanosilica refers to 20 nm silica).

The morphology of the nanosilica was characterized by Transmission Electron Microscopy (TEM). The TEM picture in Fig. 3 shows that nanosilica has uniform shape and even dispersion in the medium. Surface modification of nanosilica by the proper silane coupling agent through the hydrolysis and condensation reaction is commonly employed to yield better compatibility between the modified silica filler and the polymer matrix [16]. In this study, the liquid-phase silylation of nanosilica was performed using the epoxy resin/ethanol

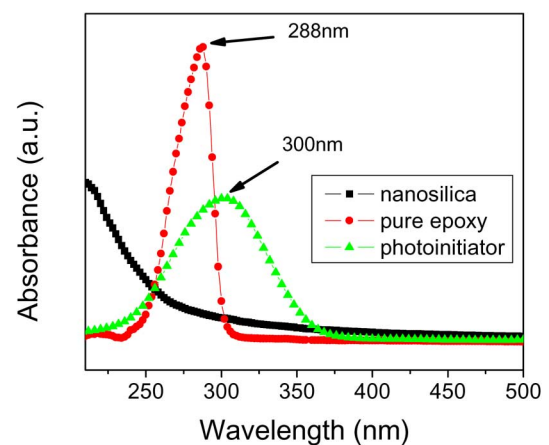


Fig. 4. UV absorbance of pure epoxy, nanosilica, and photoinitiator.

solution as a solvent. This in-situ procedure avoids the re-agglomeration of nanoparticles after modification which may occur during drying of modified nanofiller prepared in common solvents [17], [18]. To enhance the reaction rate of silane grafting, water and an organic acid as catalyst were added.

B. UV Absorption of Compositions in the Photo-Curable Nanocomposite

It has been reported that onium salts containing aromatic groups such as diaryliodonium and triarylsulphonium salts are efficient photoinitiators for cationic polymerization of epoxy. The UV-Visible spectra of photoinitiator KI85 and other compositions in the nanocomposites were characterized as shown in Fig. 4. It is noticed that, although the pure epoxy strongly absorbs UV light at a peak around 288 nm with the benzene ring in the epoxy molecular structure, the photoinitiator still can be excited in the epoxy by the UV wavelength below 360 nm due to its wide and strong UV absorption. Fig. 4 showed the influence of nanosilica addition to the UV absorption of the photoinitiator incorporated in the epoxy matrix. The two curves are almost identical except that the absorption intensity for the photo-initiator (around 325 nm) is different. With the nanosilica addition, the UV absorption intensity in the composite is reduced. This is expected to change the photo-curing kinetics of the nanocomposite, as will be shown later.

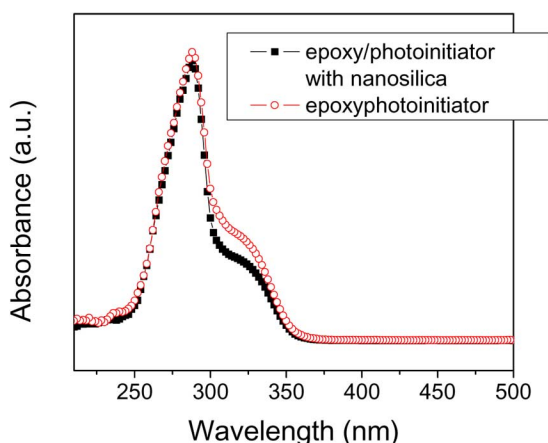


Fig. 5. Influence of nanosilica on the UV absorption of photoinitiator in epoxy.

C. Photo Curing Behavior

An important issue in preparing the nanocomposite materials was to determine whether the presence of the silica filler affected the photo-polymerization kinetics, with respect to the reaction rate and the cure extent (see Fig. 5). Therefore, photo curing experiments were performed using the photo-DSC with both the nanocomposite and a reference sample containing no fillers. Fig. 6 shows the photo-DSC curves of each sample upon UV light exposure, where the reaction heat in the photo-polymerization reaction can be calculated as the area under the curve. In the second DSC scan with thermal heating, a residue reaction peak also occurred, which indicates the photo-curing itself cannot achieve full crosslinking of the epoxy. The uncompleted curing in the photo exposure process is due to molecular mobility restrictions due to the increase in molecular weight. Once the glass transition temperature of the UV-cured composite reaches the sample temperature, the reaction stops because the polymerization can not proceed in the glassy state. Therefore, there remains a certain amount of un-reacted epoxide rings in the photo-cured nanocomposite. Table I lists the reaction heat and conversion for the nanocomposites measured by the photo-DSC. None of the samples reached 100% conversion after photo exposure, thus post-curing with high temperature is needed to increase the glass transition temperature.

From the data in Table I, it also appears that with increasing nanosilica filler loading, the conversion increases; suggesting that nanosilica with proper surface modification is providing a significant interfacial area in the matrix, resulting in a higher heat evolved in the photo-polymerization [19]. However, the curing peak time of the nanocomposite during photo-curing is delayed as the filler load increased. As mentioned before, UV light absorption intensity is reduced by filler addition, which explains the slow reaction kinetics in nanocomposites. The characterization of photoreaction behaviors of nanocomposite curing will help to determine the new process conditions when using these materials in the photolithography process due to the reaction kinetics changes.

Tgs of the nanocomposites materials after thermal curing are shown in Fig. 7. It can be seen that the addition of well-dispersed nanosilica has no significant influence on the Tg. In our previous research it was found that the Tg of nanocomposites could be

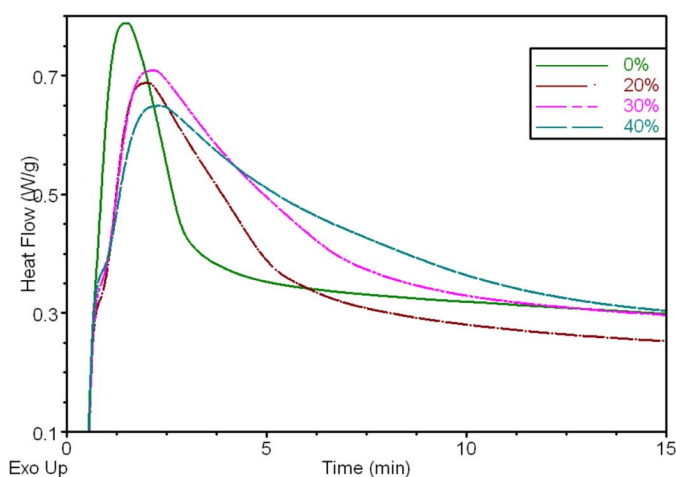


Fig. 6. Photo-DSC curves of the nanocomposite with different filler loading.

TABLE I
REACTION HEAT AND CONVERSION FOR THE
NANOCOMPOSITE MEASURED BY PHOTO-DSC

| Filler (wt %) | Reaction heat (J/g) | Conversion (%) | Peak time (min) |
|---------------|---------------------|----------------|-----------------|
| 0 | 81.4 | 56.7 | 1.1 |
| 20 | 108.3 | 75.5 | 1.88 |
| 30 | 117.9 | 81.8 | 2.19 |
| 40 | 127.8 | 88.6 | 2.26 |

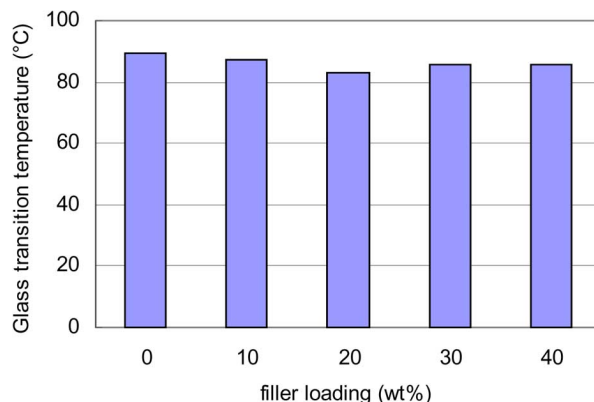


Fig. 7. DSC Tg of the nanocomposite after photo-curing followed thermal curing.

lowered by more than 30 °C if the nanofiller was not well-dispersed in the polymer matrix and had poor interfacial interaction to the polymer matrix. The current results also proved that surface modification of nanosilica is very important to achieve good filler dispersion and material properties of the nanocomposite.

D. Optical Properties

The optical properties of photo-cured nanocomposites were characterized by UV-Vis spectroscopy. Fig. 8 shows the transmittance of the nanocomposite film. After photo-curing, the absorption of the photoinitiator has disappeared due to its photolysis reaction. It can be seen that the photo-cured nanocomposites with 40wt% filler still retains excellent optical transparency (> 95%) comparable to the pure epoxy within the visible light region. The low transmittance under 350 nm is due to

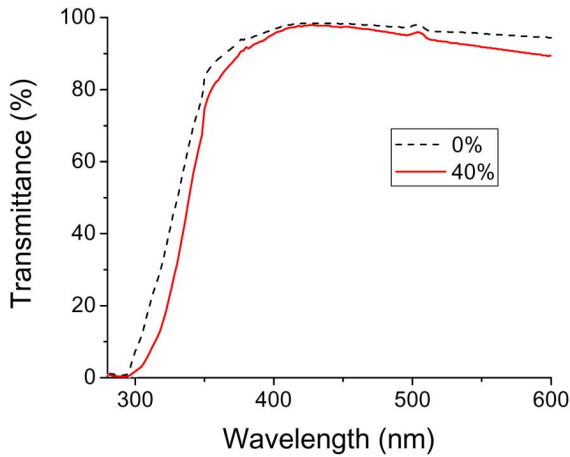


Fig. 8. Film optical properties of photo-cured nanocomposite.

the absorption of the epoxy polymer. At relatively longer wavelengths, the particle size of the nanometer-order filler is much smaller than the wavelength of light, thus less effect on the light transmission reduction is observed. Therefore, the addition of 20 nm silica has no influence on the optical properties and the nanocomposite can provide unique optical properties for wafer level applications.

E. Characterization of Photo-Cured Nanocomposites

To characterize the material properties of the epoxy/silica nanocomposite after photo-curing, the thick films were prepared by the bar-coating method with a doctor blade on an aluminum substrate. Free-standing film of nanocomposite can be obtained by peeling films from the Al substrates. The thermal mechanical properties were characterized using DMA and TMA in the film mode.

1) *Thermal Degradation Behavior*: Polymers with good thermal stability are required for microelectronic packaging applications. Fig. 9 shows the TGA curves obtained. There is a ~ 4 wt% weight decrease in the TGA curves for all the samples starting from 160 °C which is due to the evaporation of photoinitiator solvent. The photoinitiator used in the experiments was dissolved into propylene carbonate solvent which has a high boiling point of 243 °C. After this small weight loss, there are two major decomposition steps starting from around 300 °C and 550 °C, respectively. Table II shows the onset temperatures of decomposition for each sample. It can be seen that the addition of nanosilica can improve the thermal stability of pure epoxy. All the nanosilica-containing samples exhibit a larger amount of char formation than the pure epoxy sample due to the presence of filler. The exact filler loading defined as the residue in the end of TGA curve is also listed in the Table II.

2) *Thermal Expansion Properties*: The primary purpose of adding silica to the epoxy is to reduce the thermal expansion of the epoxy [5], [20]. Generally, the coefficients of thermal expansion (CTE) of composites are reduced with an increase of filler contents. Fig. 10 shows the CTE values of the nanocomposites after photo-curing. The CTE was reduced from 76.1 $\mu\text{m}/\text{m}^\circ\text{C}$ for pure epoxy to 50.2 $\mu\text{m}/\text{m}^\circ\text{C}$ after 40wt% silica addition. It is expected that with increased amounts of filler, the CTE of the

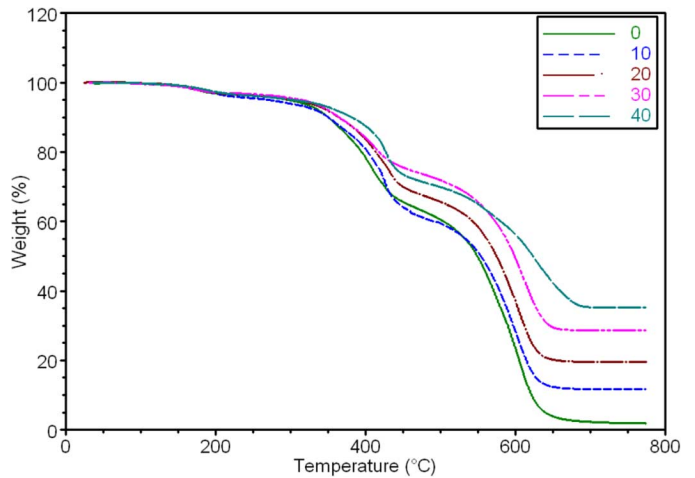


Fig. 9. TGA graphs of the photo-cured nanocomposites.

TABLE II
TGA MEASURED FOR VARIOUS FILLER LOADINGS IN THE NANOCOMPOSITES

| Sample name | 0 | 10 | 20 | 30 | 40 | |
|---|-------------|-------|-------|-------|-------|------|
| Filler (wt %) | Theoretical | 0 | 10 | 20 | 30 | 40 |
| | measured | 0 | 12 | 19.3 | 28.3 | 35.5 |
| Decomp. 1 st onset Temperature(°C) | 336.9 | 337.9 | 341.0 | 338.5 | 346.6 | |
| 2 nd onset | 545.2 | 551.9 | 556.0 | 557.3 | 576.5 | |

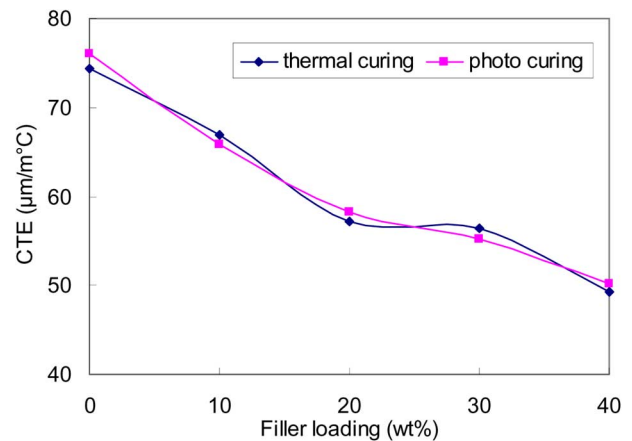


Fig. 10. Coefficient of thermal expansion of the nanocomposite.

composite can be further reduced. The CTE of the thermally cured sample is also shown in the figure. It can be seen that there is no obvious difference between the different polymerization methods in term of material thermal stability. The incorporation of the modified nanosilica can reduce the CTE and provide good dimensional stability for the composite films in this application.

3) *Thermal Mechanical Properties*: Fig. 11 shows the overlay of the storage modulus curves of the nanocomposites. With the increasing filler loading, the modulus increases almost linearly with the addition of inorganic fillers in the epoxy matrix. The DMA Tg, which was represented by the peak temperature of the tan delta curve, is also listed in Fig. 12. The Tg of the nanocomposite measured by peak temperature of tan delta showed the same trend as observed in the DSC

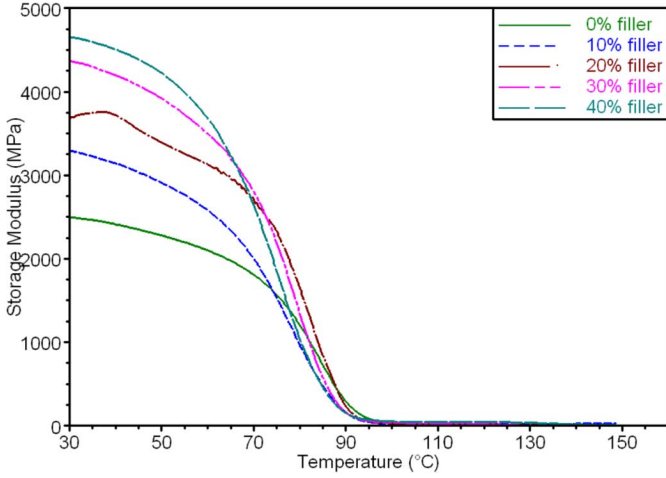


Fig. 11. DMA curves of the photo-cured nanocomposites.

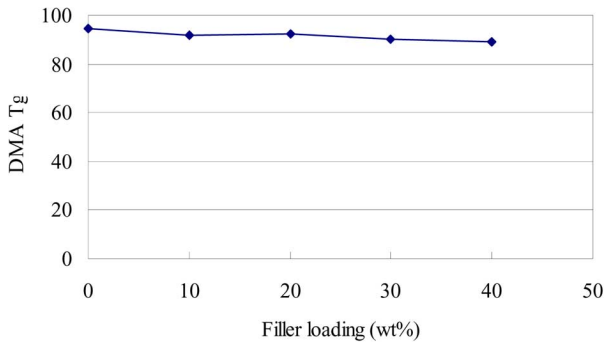


Fig. 12. Tan delta peak temperature (DMA Tg) of the photo-cured nanocomposites.

experiment, which didn't change significant as filler loading increased.

The Mori–Tanaka method [21]–[23] has been used to predict the elastic properties of two-phase composites as a function of the effective particle volume. Then, the effective Young's modulus of the composite can be derived as [24]

$$\bar{E} = 2\bar{\mu} \left[1 + \frac{3\bar{K} - 2\bar{\mu}}{2(3\bar{K} + \bar{\mu})} \right] \quad (1)$$

where

$$\bar{K} = K_0 \left\{ 1 + \frac{c(K_1 - K_0)}{K_0 + 3\gamma_0(1-c)(K_1 - K_0)} \right\} \quad (2)$$

$$\bar{\mu} = \mu_0 \left\{ 1 + \frac{c(\mu_1 - \mu_0)}{\mu_0 + 2\delta_0(1-c)(\mu_1 - \mu_0)} \right\} \quad (3)$$

$$\gamma_0 = \frac{K_0}{3K_0 + 4\mu_0} \quad (4)$$

$$\delta_0 = \frac{3(K_0 + 2\mu_0)}{15K_0 + 20\mu_0} \quad (5)$$

$$K_n = \frac{E_n}{3(1 - 2\nu_n)} \quad (6)$$

$$\mu_n = \frac{E_n}{2(1 + \nu_n)}, \quad n = 0, 1 \quad (7)$$

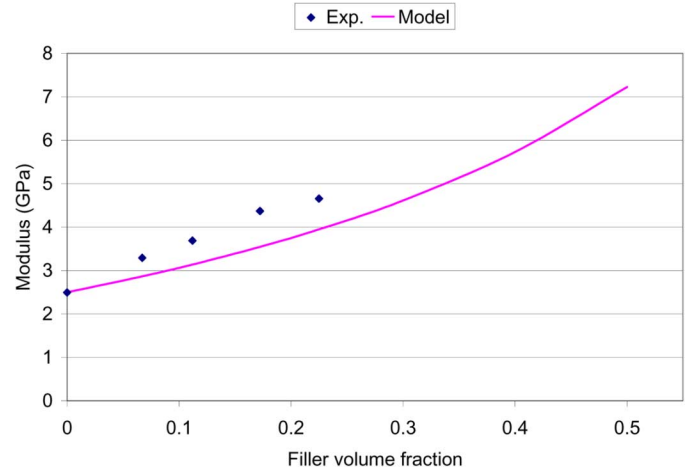


Fig. 13. Comparison of composite modulus between the theoretical prediction and experimental measurement.

TABLE III
MATERIALS CONSTANT

| | Density | Modulus (GPa) | Poisson's ratio |
|--------|--------------------------------|-------------------------|-----------------|
| epoxy | $\rho_0 = 1.16 \text{ g/cm}^3$ | $E_0 = 2.5 \text{ GPa}$ | $\nu_0 = 0.4$ |
| silica | $\rho_1 = 2.20 \text{ g/cm}^3$ | $E_1 = 74 \text{ GPa}$ | $\nu_1 = 0.19$ |

where as \bar{E} = effective bulk modulus, $\bar{\mu}$ = effective shear modulus, and c is the filler volume fraction. Young's modulus and the Poisson's ratio of the matrix are E_0 and ν_0 , that of the particles are E_1 and ν_1 .

It can be seen from the above equations that the modulus of the composite underfill is determined by the moduli of the epoxy matrix and the filler particles, as well as the particle volume fraction. Theoretically, once these parameters are given, these equations can be used as a tool to estimate the modulus of the composite underfill. Based on the materials properties (Table III), the predicted modulus of composite from Mori–Tanaka method was compared with the measured results (Fig. 13).

Previous research had validated the Mori–Tanaka model for the composite filled with the micron size filler, in which the agreement between the theoretically predicted and experimentally measured modulus was excellent [25]. Nevertheless, the prediction showed a large deviation from the experimental results of our results, as shown in Fig. 13, which implied the limitation of Mori–Tanaka model for the nanocomposites. This model assumed that only two phases exist (matrix and filler), and they are perfectly bonded to each other. This assumption may work well for the reinforcements of polymer matrix with the micron-sized filler, or higher. However, for nanocomposites, it has been shown that the molecular structure of the polymer matrix is significantly perturbed at the filler/polymer interface, and this may create a third phase, interphase [26]. Therefore, the reinforcement of nanocomposite is not accurately described as consisting of just two phases, thus the Mori–Tanaka model is not expected to perform well for nanocomposite. More research needs to be done based on the effective interface model of the nanocomposite structure [23].

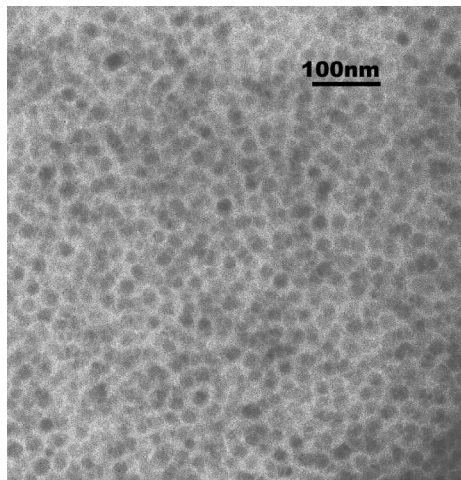


Fig. 14. TEM picture of nanocomposite after photo-curing.

4) *Nanocomposite Morphology*: Fig. 14 contains a TEM picture that shows the nanocomposite morphology with 30wt% filler loading. Note that the nanosilica is well dispersed in the polymer matrix after photo-curing. No particle agglomerations or clusters were observed which indicates good compatibility of the nanosilica surface with the polymer matrix after surface modification. Therefore, any problems associated with filler agglomerations were eliminated.

IV. CONCLUSION

The 20-nm colloidal silica after proper surface modification showed excellent optical transparency and was therefore chosen as the filler to reduce the thermal expansion of photo-curable epoxy material. UV-Visible spectrum results showed the addition of nanosilica had no influence on the photoinitiator absorption in the epoxy and the material optical properties after photo-curing. The photo-curing process of nanocomposites was studied by photo-DSC. The crosslinking of materials increased as the filler loading increase using UV exposure, but post-thermally curing was still necessary to achieve fully crosslinking of the epoxy, as shown in the both photo- and thermal-DSC experiments. Other material properties, such as thermal stability and thermal mechanical properties were also improved after nanosilica addition.

REFERENCES

- [1] Z. Zhang, Y. Sun, L. Fan, and C. P. Wong, "Study on B-stage properties of wafer level underfills," *J. Adh. Sci. Technol.*, vol. 18, pp. 361–380, 2004.
- [2] E. H. Conradie and D. F. Moore, "SU-8 thick photoresist processing as a functional material for MEMS applications," *J. Micromech. Microeng.*, vol. 12, pp. 368–374, 2002.
- [3] P. Lall, S. Islam, J. Suhling, and G. Tian, "Nano-Underfills for high-reliability applications in extreme environments," in *Proc. Electron. Comp. Technol. Conf.*, 2005, pp. 212–222.
- [4] Y. P. Zheng, Y. Zheng, and R. C. Ning, "Effects of nanoparticles SiO₂ on the performance of nanocomposites," *Mater. Lett.*, vol. 57, pp. 2940–2944, 2003.
- [5] S. Kang, S. I. Hong, C. R. Choe, M. Park, S. Rim, and J. Kim, "Preparation and characterization of epoxy composites filled with functionalized nanosilica particles obtained via sol-gel process," *Polymer*, vol. 42, pp. 879–887, 2001.

- [6] S. G. Konsowski and A. R. Helland, *Electronics Packaging of High Speed Circuitry*. New York: McGraw-Hill, 1997.
- [7] K. K. Baikerikar and A. B. Scranton, "Photopolymerizable liquid encapsulants for microelectronic devices," *Polymer*, vol. 42, pp. 431–441, 2001.
- [8] F. Bauer, H. Ernst, D. Hirsch, S. Naumov, M. Pelzing, V. Sauerland, and R. Mehnert, "Preparation of scratch and abrasion resistant polymeric nanocomposites by monomer grafting onto nanoparticles," *Macromol.Chem.Phys.*, vol. 205, pt. 5, pp. 1587–1593, 2004.
- [9] J. Zhang, K. L. Tan, G. D. Hong, L. J. Yang, and H. Q. Gong, "Polymerization optimization of SU-8 photoresist and its applications in microfluidic systems and MEMS," *J. Micromech. Microeng.*, vol. 11, pp. 20–26, 2001.
- [10] K. K. Tung, W. H. Wong, and E. Y. B. Pun, "Polymeric optical waveguides using direct ultraviolet photolithography process," *Appl. Phys. A-Mater. Sci. Process.*, vol. 80, pp. 621–626, 2005.
- [11] J. Liu, *Conductive Adhesives for Electronics Packaging*. Isle of Man, U.K.: Electrochemical Publications, 1999.
- [12] T. Naganuma and Y. Kagawa, "Effect of particle size on the optically transparent nano meter-order glass particle-dispersed epoxy matrix composites," *Compos. Sci. Technol.*, vol. 62, pp. 1187–1189, 2002.
- [13] Y. Sun, Z. Zhang, and C. P. Wong, "Study and characterization on the nanocomposite underfill for flip chip applications," *IEEE Trans. Compon. Packag. Technol.*, vol. 29, no. 1, pp. 190–197, Mar. 2006.
- [14] Y. Sun, Z. Zhang, and C. P. Wong, "Study on mono-dispersed nanosize silica by surface modification for underfill applications," *J. Coll. Interf. Sci.*, vol. 292, pp. 436–444, 2005.
- [15] Y. L. Liu, C. Y. Hsu, W. L. Wei, and R. J. Jeng, "Preparation and thermal properties of epoxy-silica nanocomposites from nanoscale colloidal silica," *Polymer*, vol. 44, pp. 5159–5167, 2003.
- [16] M. Q. Zhang, M. Z. Rong, S. L. Yu, B. Wetzel, and K. Friedrich, "Effect of particle surface treatment on the tribological performance of epoxy based nanocomposites," *Wear*, vol. 253, pp. 1086–1093, 2002.
- [17] H.-J. Glasel, F. Bauer, H. Ernst, M. Findeisen, E. Hartmann, H. Langguth, R. Mehnert, and R. Schubert, "Preparation of scratch and abrasion resistant polymeric nanocomposites by monomer grafting onto nanoparticles, 2 characterization of radiation-cured polymeric nanocomposites," *Macromol.Chem.Phys.*, vol. 201, pp. 2765–2770, 2000.
- [18] M. Fujiwara, K. Kojima, Y. Tanaka, and R. Nomura, "A simple preparation method of epoxy resin/silica nanocomposite for T-g loss material," *J. Mater. Chem.*, vol. 14, pp. 1195–1202, 2004.
- [19] F. M. Uhl, S. P. Davukuri, S.-C. Wong, and D. C. Webster, "Polymer films possessing nanoreinforcements via organically modified layered silicate," *Chem. Mater.*, vol. 16, pp. 1135–1142, 2004.
- [20] T. J. Pinnavaia and G. W. Beall, *Polymer-Clay Nanocomposite*. New York: Wiley, 2000.
- [21] T. Mura, *Micromechanics of Defects in Solids*. New York: Martinus Nijhoff, 1987.
- [22] T. Mori and K. Tanaka, "Average stress in matrix and average elastic energy of materials with misfitting inclusions," *Acta Metallurgica*, vol. 21, pp. 571–574, 1973.
- [23] G. M. Odegard, T. C. Clancy, and T. S. Gates, "Modeling of the mechanical properties of nanoparticle/polymer composites," *Polymer*, vol. 46, pp. 553–562, 2005.
- [24] J. Qu, "Effects of slightly weakened interfaces on the overall elastic properties of composite materials," *Mech. Mater.*, vol. 14, pp. 269–281, 1993.
- [25] J. Qu and C. P. Wong, "Effective elastic modulus of underfill material for flip-chip applications," *IEEE Trans. Compon. Packag. Technol.*, vol. 25, pp. 53–55, 2002.
- [26] G. M. Odegard, T. S. Gates, K. E. Wise, C. Park, and E. J. Siochi, "Constitutive modeling of nanotube-reinforced polymer composites," *Compos. Sci. Technol.*, vol. 63, pp. 1671–1687, 2003.



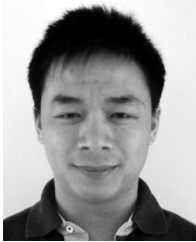
Yangyang Sun (S'07) received the B.S and M.S. degrees from Shanghai Jiao Tong University, Shanghai, China, in 1998 and 2001, respectively, and is currently pursuing the Ph.D. degree at the Georgia Institute of Technology, Atlanta.

Her research focuses on the application of nanocomposite materials in electronics packaging.



Hongjin Jiang received the B.S. and M.S. degrees from Fudan University, Shanghai, China, in 2000 and 2003, respectively, and is currently pursuing the Ph.D. degree at the Georgia Institute of Technology, Atlanta.

His research focuses on the application of nano lead-free solder in electronics packaging.



Lingbo Zhu received the B.S. and M.S. degrees in chemical engineering from East China University of Science and Technology, Shanghai, in 1999 and 2002, respectively, and is currently pursuing the Ph.D. degree in chemical engineering at the Georgia Institute of Technology, Atlanta.

His research interests include synthesis of 1-D nanomaterials, their applications in electrical interconnects and thermal managements in micro-electronic devices, and MEMS fabrication.



C.P. Wong (SM'87–F'92) received the B.S. degree in chemistry from Purdue University, West Lafayette, IN, and the Ph.D. degree in organic/inorganic chemistry from Pennsylvania State University, University Park.

He is a Regents' Professor and the Charles Smithgall Institute Endowed Chair at the School of Materials Science and Engineering, Georgia Institute of Technology, Atlanta. After his doctoral study, he was awarded a two-year postdoctoral fellowship with Nobel Laureate Professor Henry Taube at Stanford University, Stanford, CA. He joined AT&T Bell Laboratories in 1977 and became a Senior Sember of the Technical Staff in 1982, a Distinguished Member of the Technical Staff in 1987, and was elected an AT&T Bell Lab Fellow in 1992. Since 1996, he has been a Professor at the School of Materials Science and Engineering, Georgia Institute of Technology. He was named a Regents' Professor in July 2000, elected the Class of 1935 Distinguished Professor in 2004 for his outstanding and substained contributions in research, teaching and services, and named holder of the Georgia Tech Institute Endowed Chair in 2005. His research interests lie in the fields of polymeric materials, materials reaction mechanism, IC encapsulation, in particular, hermetic equivalent plastic packaging, electronic manufacturing packaging processes, interfacial adhesions, and nano functional material syntheses and characterizations.

Dr. Wong received the AT&T Bell Labs Fellow Award in 1992, the IEEE CPMT Society Outstanding and Best Paper Awards in 1990, 1991, 1994, 1996, 1998, and 2002, the IEEE CPMT Society Outstanding Sustained Technical Contributions Award in 1995, the Georgia Tech Sigma Xi Faculty Best Research Paper Award in 1999, the Best M.S., Ph.D., and undergraduate Theses Award in 2002 and 2004, respectively, the University Press (London) Award of Excellence, the IEEE Third Millennium Medal in 2000, the IEEE EAB Education Award in 2001, the IEEE CPMT Society Exceptional Technical Contributions Award in 2002, and the IEEE CPMT Field Award in 2006. He is a Fellow of AIC and AT&T Bell Labs and a member of the National Academy of Engineering. He was the Technical Vice President (1990 and 1991) and the President of the IEEE CPMT Society (1992 and 1993).